Development and In Vitro Evaluation of a Zerumbone Loaded Nanosuspension Drug Delivery System

Shadab Md [1],*, Bradon C.M Kit [2], Sumeet Jagdish [2], Dexter J.P David [2], Manisha Pandey [1] and Lipika Alok Chatterjee [1]

[1] Department of Pharmaceutical Technology, School of Pharmacy, International Medical University (IMU), Kuala Lumpur 57000, Malaysia; manishapandey@imu.edu.my (M.P.); Chatterjee.lipika@gmail.com (L.A.C.)

[2] BPharm, School of Pharmacy, International Medical University (IMU), Kuala Lumpur 57000, Malaysia; brandon.choy@student.imu.edu.my (B.C.M.K.); Sumeet.jagdish@student.imu.edu.my (S.J.); Dexter.david@student.imu.edu.my (D.J.P.D.)

* Correspondence: shadabmd1982@gmail.com

Abstract: Zerumbone extracted from the volatile oil of rhizomes available from the *Zinigiber zerumbet* has promising pharmacological activity. However, it has poor aqueous solubility and dissolution characteristics. To improve this, a nanosuspension formulation of zerumbone was developed. Nanosuspensions were formulated using high-pressure homogenization (HPH) with sodium dodecyl sulphate (SDS) and hydroxypropylmethylcellulose (HPMC) as stabilizers; the formulation was optimized and freeze dried. The optimized nanosuspension product was evaluated using an optical light microscope, photon correlation spectroscopy (PCS), polydispersity index, zeta potential, SEM, differential scanning calorimetry (DSC) and FT-IR. The physical stability of the nanosuspensions was evaluated for 30 days at 4 °C, 25 °C, and 37 °C. To validate the theoretical benefit of the increased surface area, we determined an in vitro saturation solubility and dissolution profile. The mean particle size, polydispersity index and zeta potential of the zerumbone nanosuspensions stabilized by SDS versus HPMC were found to be 211 ± 27 nm vs. 398 ± 3.5 nm, 0.39 ± 0.06 vs. 0.55 ± 0.004, and −30.86 ± 2.3 mV vs. −3.37 ± 0.002 mV, respectively. The in vitro saturation solubility and dissolution revealed improved solubility for the zerumbone nanosuspension. These results suggested that the nanosuspensionlization improves the saturation solubility and dissolution profile of zerumbone, which may facilitate its use as a therapeutic agent in the future.

Keywords: zerumbone; nanosuspension; sodium dodecyl sulphate; dissolution study; short term stability

1. Introduction

An estimated 80% of the world population relies on traditional therapies, mostly involving the use of natural compounds. Zerumbone is classified as a sesquiterpernoid that is present in the essential volatile oil of rhizomes available from the edible wild ginger, *Zinigiber zerumbet* [1]. The chemical structure of zerumbone contains two conjugated and one isolated double bonds, α,β-unsaturated carbonyl group, and a double conjugated carbonyl group in the 11-membrane ring structure. The molecular formula for zerumbone is $C_{15}H_{24}O_2$ (Figure 1) [2,3]. It is completely soluble in ethanol and dimethyl sulfoxide but poorly soluble in water (1.296 mg/L at 25 °C) [4]. Zerumbone has been shown to possess strong in vitro antitumor activity in cell lines. In this context Abdul et al. evaluated the anticancer and antimicrobial activity of zerumbone and they found that zerumbone showed antibacterial activity on *S. choleraesuis*, however no antifungal activity was observed, Moreover, it exerted an antiproliferative effect on HeLa cells [5]. Similarly, Sidahmed et al.

evaluated the gastroprotective effect of zerumbone and the results depict that zerumbone promotes ulcer protection along with antioxidant activity and maintenance of mucus integrity [6]. It also has been shown to have anti-inflammatory and antioxidant properties [7]. Despite having promising pharmacological activities, its clinical development has been hindered because of its poor aqueous solubility and consequent low bioavailability. Nanosuspension is one strategy used to improve oral bioavailability of poorly soluble drugs [8]. One approach to producing nanosuspensions is using the top-down technique, in which the large drug particles are broken down into smaller ones (i.e., nanosuspensions) by using high-pressure homogenisation (HPH). The resultant nanosuspensions are of a nanometre size and have a high surface area to volume ratio [9]. The nanoparticles are stabilized in an aqueous medium using stabilizer that are generally recognized as safe [10]. Post-manufacturing processing is undertaken using freeze or spray drying with cryoprotectants to maintain the integrity of the nanoparticles and prolong their shelf life [11]. The size of a nanosuspensions improves the saturation solubility and dissolution rate of the drug, leading to an increase in oral bioavailability. Apart from improved bioavailability, nanosuspensions also offer enhanced stability, reduced systemic toxicity and increased pharmacodynamic action [12]. Since the introduction of nanosuspension technology in 1992, the first product approved by the Food and Drug Administration (FDA) for oral delivery in 2000 was sirolimus (Rapamune®) an immunosuppressive agent [13]. Currently, there are more than twenty approved products on the market, which is growing fast, due the potential of this technology [14].

This is the first time we are reporting the formulation of zerumbone nanosuspensions. In the present study, zerumbone nanosuspensions were formulated using the high pressure homogenisation (HPH) method. Two stabilizers, sodium dodecyl sulphate and hydroxypropylmethylcellulose (HPMC), were chosen which could improve the solubility of the product, which was optimised, characterised, and assessed for short-term stability.
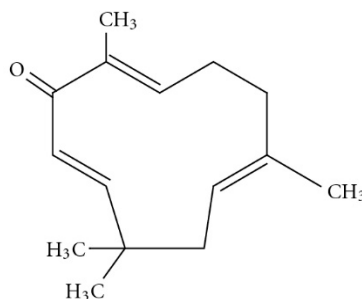
Figure 1. Chemical structure of zerumbone (adopted from [3]).

2. Materials and Methodology

2.1. Materials

The zerumbone was extracted at IMU research Lab, Malaysia. The hydroxypropylmethylcellulose (HPMC) and sodium dodecyl sulphate (SDS) were purchased from LabChem (Petaling Jaya, Malaysia). The lactose was purchased from R&M Chemicals Malaysia, and was utilized as a cryoprotectant for freeze drying. All of the other reagents and chemicals used were of analytical grade.

2.2. Preparation of Nanosuspensions

The zerumbone nanosuspensions were prepared using the HPH method. Of the zerumbone, 500mg was dispersed in 100 mL HPMC and SDS solution (0.1%, *w/v*) under magnetic stirring for an hour. The mixture was then disintegrated into microparticles using an Ultra-Turrax® T25 Basic (IKA-Werke, Breisgau, Germany) at 20,000 rpm for 5 min, followed by 6 pre-milling homogenisation cycles at 800 bar through a high-pressure homogeniser (EmulsiFlex-C3; Avestin Inc., Ottawa, ON,

Canada). HPH was then applied for 30 cycles at 1500 bar. Samples were collected after pre-milling, and after 1, 5, 10, 15, 20, and 30 cycles at 1500 bar. The optimised product was freeze-dried with lactose as a cryoprotectant in ScanVac Coolsafe Freeze Dryer (LaboGene, Lillerød, Denmark) for 72 h. The freeze-dried nanosuspensions were re-dispersed in water before analysis.

3. Characterisation and Evaluation of Nanosuspension

3.1. Particle Size, Size Distribution and Zeta Potential Analysis

The average particle size and particle size distribution (PDI) analysis were determined using photon correlation spectroscopy (Zetasizer Nano ZS; Malvern Instruments, Worcestershire, UK). The ZP was evaluated by determining the particle electrophoretic velocity using the Zetasizer Nano. All of the samples were diluted with distilled water (1:10) to be ready for collecting the final experimental values in the triplicates.

3.2. Morphology of Freeze-Dried Nanosuspensions

The morphology of the zerumbone nanosuspensions was observed under a light microscope (Leica DMLS Microscope; Reichert Inc., Depew, NY, USA). The scanning electron microscopy (SEM) was conducted at different magnifications after being sputter-coated with gold on a sample holder and dried in vacuum (TM3000 Tabletop Scanning Electron Microscope; Hitachi, Tokyo, Japan).

3.3. Fourier Transform Infrared Spectroscopy (FT-IR)

The FT-IR spectra were recorded using IRAffinity-1S FT-IR spectrometer (Shimadzu, Kyoto, Japan). The FT-IR measurements were performed in the scanning range of 4000–500 cm^{-1} at room temperature by KBr pellet method. The FT-IR spectra of the nanosuspensions were compared with zerumbone, and physical mixture.

3.4. Differential Scanning Calorimetry (DSC)

The thermal characteristics of zerumbone, physical mixture, and nanosuspensions were determined using a differential scanning calorimeter (DSC823e; Mettler Toledo, Greifensee, Switzerland). The samples were weighed, sealed in a 40 μL aluminium pan, and heated from 20–80 °C at 5 °C/min under constant flow of dry nitrogen.

3.5. Saturation Solubility

For the measurement of the saturation solubility of free drug of zerumbone, 50 mg drug was dispersed in 5 mL of distilled water and stirred by a magnetic stirrer at 700 rpm for 24 h. Of this dispersion, 1.5 was extracted and centrifuged at 25,000 rpm for 30 min at 25 °C. The supernatant was analysed spectrophotometrically at 254 nm after suitable dilution with methanol and water (1:4) using UV-visible spectrophotometer. Similarly, the saturation solubility of the zerumbone nanosuspension in the form of nanoemulsion was evaluated by taking nanoemulsion equivalent to 50 mg of zerumbone. For the measurement of saturation solubility of the nanosuspension of zerumbome, the concentration of zerumbone was calculated from a standard curve in the methanol.

Standard Curve of Zerumbone

The Stock solution of zerunbone was prepared by dissolving 5 mg of drug in a sufficient amount of methanol and to top it to 50 mL. To make standard solution, take separately 2.5, 5, 10 and 20 mL from the stock solution and dissolve it separately in methanol to make the final volume up to 10 mL. The absorbance for each solution using a UV spectrophotometer at wavelength 254 nm was noted and a graph of absorbance (along x-axis) against concentration (along y-axis) was constructed.

### 3.6. In Vitro Dissolution Testing

The dissolution studies were carried out using activated dialysis tubing and phosphate buffered saline (pH 7.4) as the dissolution medium. Then 2 mg of zerumbone or zerumbone nanosuspension was dissolved in 0.2 mL of distilled water and was added into the dialysis tubing. The dialysis tubing was immersed in a beaker on a hotplate stirrer adjusted to 37 °C and rotated at a speed of 100 rpm. At different time intervals (5, 15, 30, 60 and 120 min), 3 mL samples were withdrawn and filtered using a 0.22 μm membrane filter, followed by a compensation with the same volume of fresh dissolution medium. The absorbance of the samples were measured using UV/Vis spectrometer at a wavelength of 254 nm using phosphate buffer saline (pH 7.4) as the blank. The percentage of drug released was calculated by the following:

$$\text{Percentage drug released } = \frac{\text{concentration of naringenin(mg/mL)} \times \text{ dissolution bath volume(mL)}}{\text{Amount of naringenin in dialysis bag (mg)}} \times 100$$

4. Results and Discussion

4.1. Preparation and Optimisation of Nanosuspension

The HPH technique was used in the preparation of the zerumbone nanosuspensions. Stabilisers were added to nanosuspension formulations to diminish the free energy of the system by diminishing the interfacial tension as well as to prevent the nanoparticle aggregation through the electrostatic/steric stabilisation [15]. Polymeric (HPMC) and surfactant (SDS) based stabilisers were chosen in this study because the adsorbed polymer and surfactants layers are more robust and can prevent aggregation [16]. A pre-milling procedure was performed to reduce the large crystals in the suspension prior to subjecting them to high pressure homogenisation. This prevents the large crystals from blocking the homogenisation gap present in the piston gap homogenizer [17]. The pressure for the high-pressure homogeniser was set at 1500 bar and the sample was passed through for 30 cycles. Figures 1 and 2 show the decrease in particle size and PDI respectively, and the increase in ZP as the number of homogenisation cycles increases. It has been shown that increasing the pressure beyond 2000 bar has little effect in further decreasing the particle size; thus 1500 bar up to 30 homogenisation cycles were chosen for this study. Cycle 20 was chosen as the optimised cycle as it yielded the lowest particle size and PDI compared with the other cycles. Further cycles were not needed as the particle size difference was not significant. The optimisation was based on the characterisation parameters which would yield the smallest particle size, lowest PDI and highest zeta potential. Figure 2 reveals that the most pronounced particle size reduction took place on cycle 20 for the (zerumbone: SDS) 5:1 formulation. A similar observation was observed with the (zerumbone: SDS) 1:1 formulation on cycle 15 for the (data not shown). The profile of the particle size reduction and PDI was similar in both of the ratios (data not shown); however, the 5:1 stabilizer drug formulation displayed slightly reduced particle size. The zeta potentials for both of the formulations were around −30 mV, which indicates that they may be stable for short to long term [18]. Increases in the homogenisation cycles did not reduce the particle size in either case. This is because of the input of energy during the homogenisation process leading to aggregation, as evident by the PDI readings. Even though both of the formulation ratios displayed satisfactory readings before cycle 15, it is recommended to take the parameters into account after cycle 10, as evidence suggests that the formulations would become unstable later [12]. Therefore, the 5:1 formulation cycle 20 was chosen to be optimised further in this case, as it showed reduced particle size as compared the 1:1 cycle 15 (184.0 nm vs. 247.5 nm for zerumbone nanosuspension stabilized by SDS) whereas the PDI and zeta potential for both of the formulations were similar and desirable. A similar pattern was observed with the nanosuspensions stabilised by HPMC, however the obtained particle size was much larger with alow zeta potential compared to the zerumbone nanosuspension stabilized by SDS (Figure 3A,B).
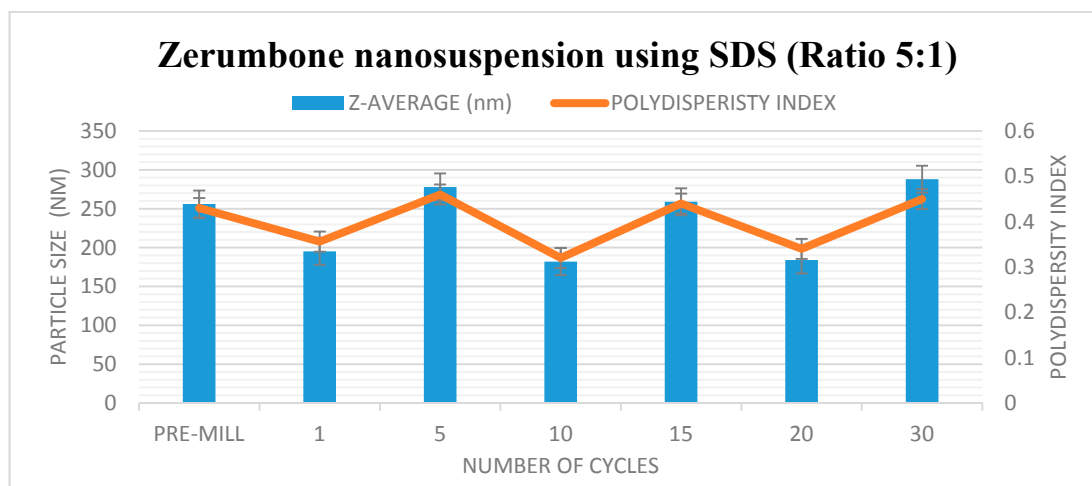
Figure 2. Decrease in particle size and size distribution (presented as polydispersity index (PI) as a function of the homogenization cycles for the zerumbone nanosuspensions stabilized by sodium dodecyl sulphate (SDS).
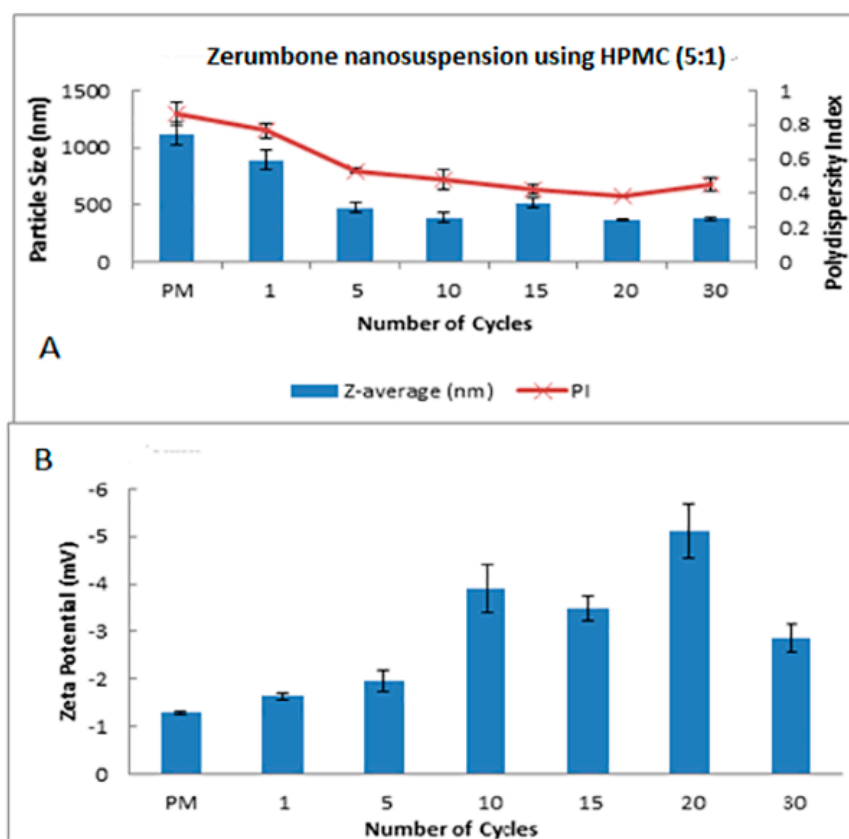

Figure 3. Decrease in the particle size and size distribution (presented as polydispersity index (PI) (**A**) and the zeta potential (**B**) as a function of the homogenization cycles for the zerumbone nanosuspensions stabilized by hydroxypropylmethylcellulose (HPMC).

4.2. Characterization and Evaluation of Nanosuspension

4.2.1. Particle Size and Zeta Potential Analysis

The optimised zerumbone nanosuspensions stabilized by SDS displayed an average size of 211 ± 27 nm with the PDI of 0.39 ± 0.06 and zeta potential of −30.86 ± 2.3 mV. The optimised zerumbone nanosuspensions stabilized by HPMC showed an average particle size of 398 ± 3.5 nm with a PI of 0.55 ± 0.004 and ZP of −3.37 ± 0.002 mV. For the nanosuspension to be stable, apart from having a PDI less than 0.5 and zeta potential more than −30 mV, a uniform particle size distribution is vital. Having a broad size distribution in the system can result in the aggregation of particles and can dramatically affect its stability [10]. The size distribution analysis of the zerumbone nanosuspension stabilized by SDS revealed a sharp strong intense peak, showing more than 80% of nanoparticles in the system were around 200 nm (Figure 4A), whereas zerumbone nanosuspensions stabilized by HPMC 80% of the nanoparticles' sizes were approximately 400 nm (Figure 4B).
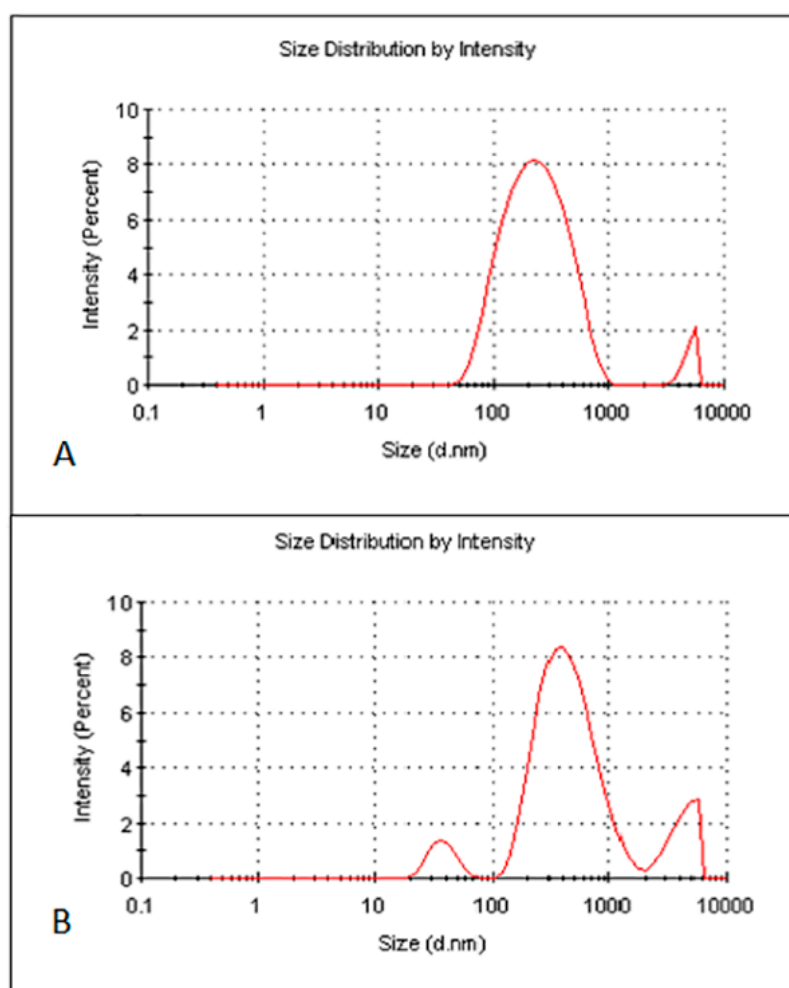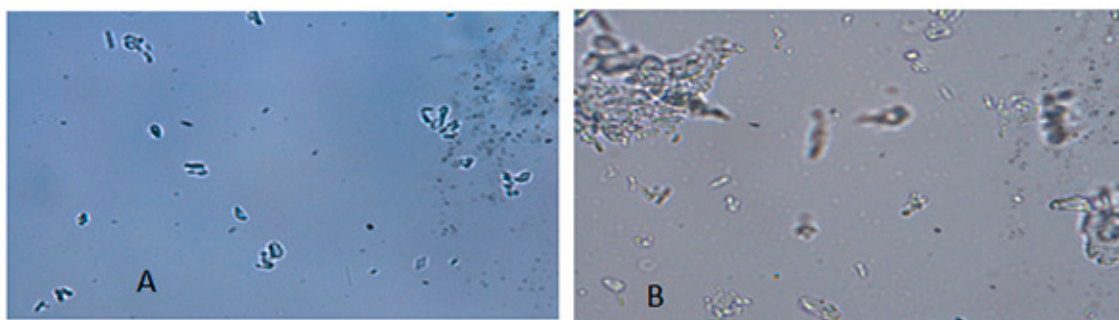

Figure 4. Particle size and size distribution of optimised freeze dried SDS-zerumbone nanosuspensions (**A**) and freeze dried HPMC-zerumbone nanosuspensions (**B**).

4.2.2. Morphology Analysis

The morphology of the freeze-dried nanosuspensions was observed under the optical light microscope and SEM. The individual crystals were mostly observed under a light microscope after the nanosuspensions were re-dispersed in water (Figure 5A). In the case of the zerumbone nanosuspensions stabilized by SDS, aggregation was not observed; this could be due to the high zeta potential.

However, in case of zerumbone nanosuspensions stabilized by HPMC, aggregated crystals were observed, probably because of the low zeta potential. The SEM images of both of the nanosuspension formulations displayed aggregated particles because of the water-removal (Figure 6A,B). A probable explanation behind this could be due to the capillary forces experienced during the freeze drying which leads to aggregation [13].


Figure 5. Micrographs (×1000 magnification) of freeze dried SDS-zerumbone nanosuspensions (**A**) and freeze dried HPMC-zerumbone nanosuspensions (**B**).

(**A**)   (**B**)
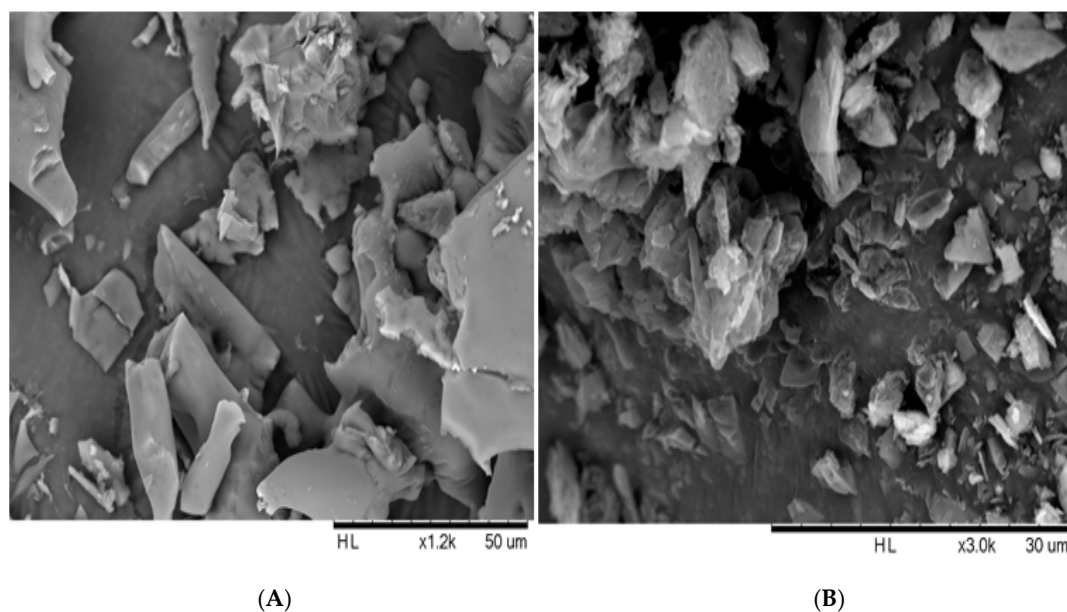
Figure 6. SEM image of freeze dried SDS-zerumbone nanosuspensions (**A**) and freeze dried HPMC-zerumbone nanosuspensions (**B**).

4.2.3. Differential Scanning Calorimetry

The high energy input during the nanosizing may induce changes in the crystallinity state; this could possibly lead to the formation of amorphous particles [10]. The DSC thermograms revealed a single endothermic peak at 67 °C for both zerumbone and its physical mixture (Figure 7). On the other hand, no endothermic peak was observed in the case of the zerumbone nanosuspensions (Figure 7) suggesting that the nanosizing process affected the crystalline state of the nanosuspensions to be partially or fully amorphous.
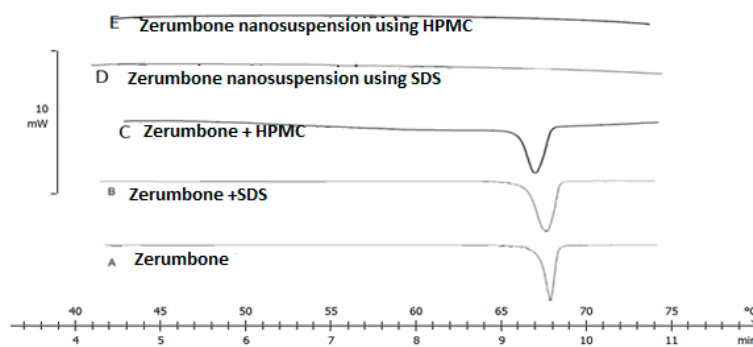
Figure 7. DSC thermograms of freeze dried (**A**) zerumbone, (**B**) zerumbone and SDS physical mixture, (**C**) zerumbone and HPMC physical mixture, (**D**) SDS-Zerumbone nanosuspensions (**E**) freeze dried HPMC-zerumbone nanosuspensions.

4.2.4. Fourier Transforms Infrared Spectroscopy (FT-IR)

FT-IR was used to evaluate the interaction between stabiliser and drug. The FT-IR spectra of the zerumbone, SDS and HPMC physical mixtures and nanosuspensions were taken (Figure 8). The characteristic peak for zerumbone can be detected at 1650 cm^{-1} which shows the presence of $\alpha\beta$-unsaturated ketone [19]. Zerumbone and its physical mixture displayed comparable FTIR spectra, as the characteristic peak was identified at 1650 cm^{-1}. Conversely, this peak was not detected in the FTIR spectrum of the nanosuspensions, which may indicate the alteration of chemical structure during the nanosizing process.
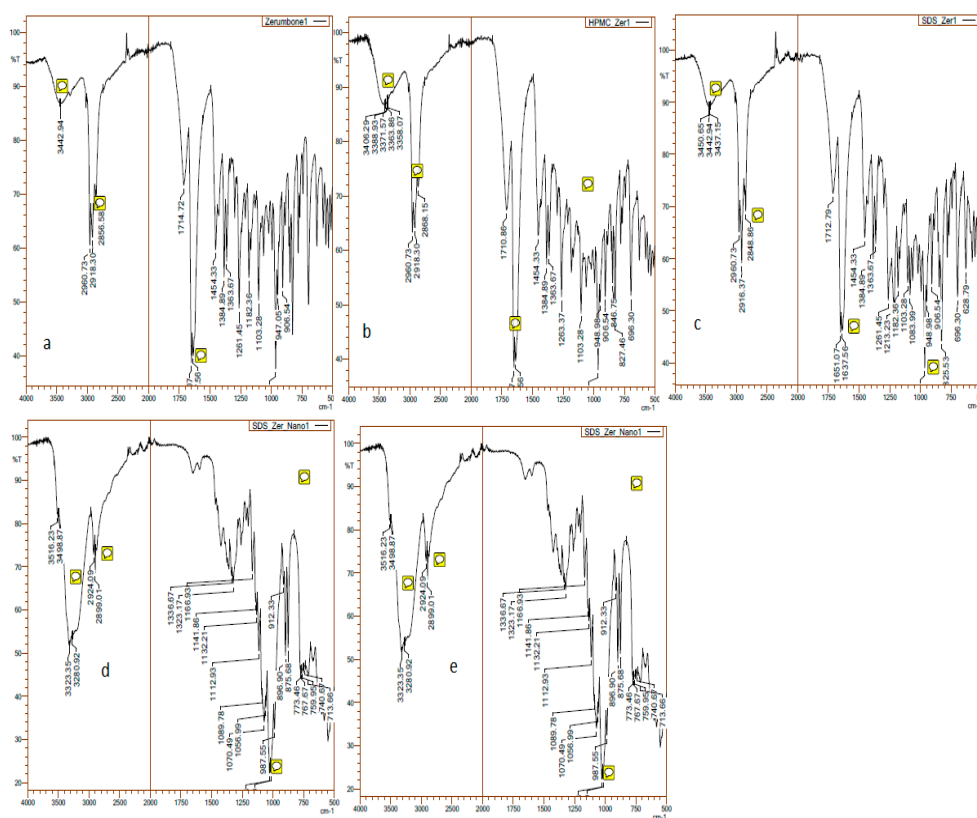

Figure 8. FTIR of the (**a**) zerumbone; (**b**) zerumbone and SDS physical mixture; (**c**) zerumbone and HPMC physical mixture, tand; (**d**) SDS-zerumbone nanosuspensions; (**e**) freeze dried HPMC-zerumbone nanosuspensions at 4000 cm^{-1} to 500 cm^{-1}.

4.3. Physical Stability

4.3.1. Physical Stability of Zerumbone Nanosuspension Stabilized by SDS

The freshly prepared, optimized nanosuspensions were stored at 4 °C, 25 °C, and 37 °C for 30 days to measure the short-term stability. The particle size, PDI and zeta potential remained very much similar throughout the storage period (Figure 9). The zeta potential remained nearly the same (-30.86 ± 2.3 mV) for all three of the storage conditions. For the nanosuspension to be stable for short term, a zeta potential of at least -20 mV is required and -30 mV is required for long term stability [20]. In this case, the zeta potential on day 0 was -33.27 mV, therefore predicting that the nanosuspension would be stable. Furthermore, the PDI was less 0.5 throughout indicating that the width of the distribution among the nanoparticles is sufficient enough to prevent aggregation [8]. Overall, particle size remained nearly stable throughout; however, there was a slight increase in particle size for all three of the storage conditions and a reduction on day 30 to around 150 nm from the original 200 nm. This may be related to a drug-stabiliser interaction rather than a temperature effect, as the same pattern was observed under all three of the storage conditions. High molecular weight stabilisers, such as SDS, can result in micellar transformation over a period of time, which may result in either an increase or a decrease in the particle size of the drug in question [21].
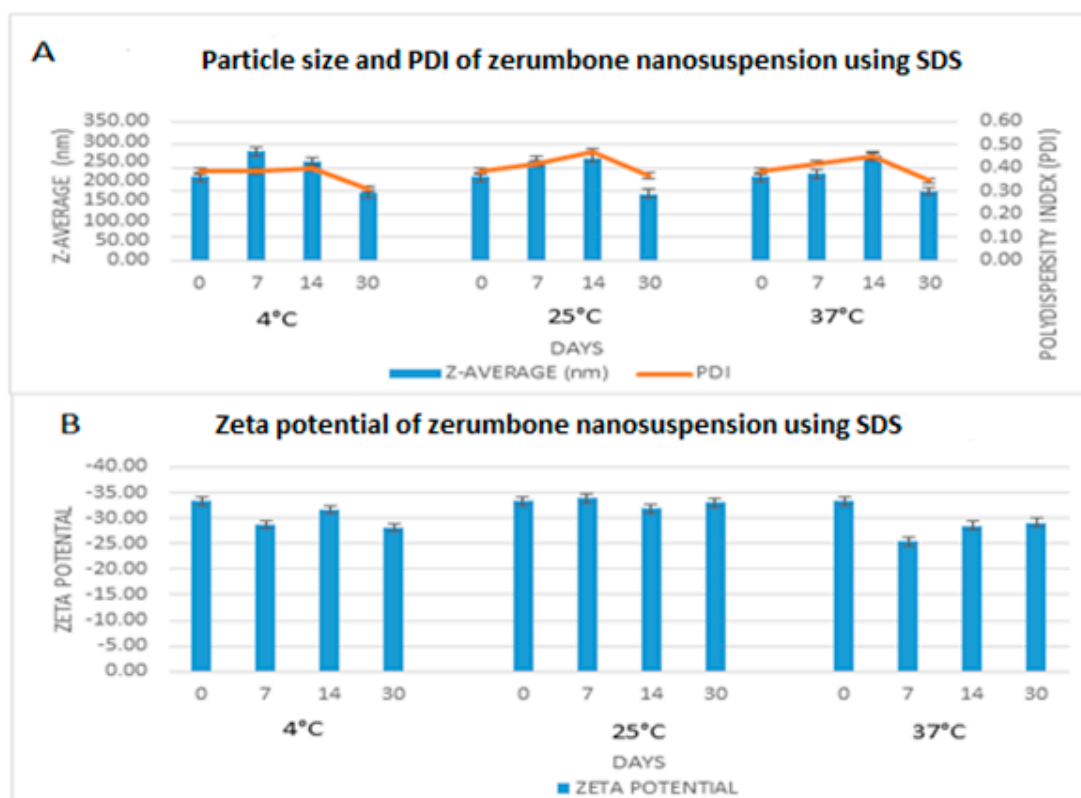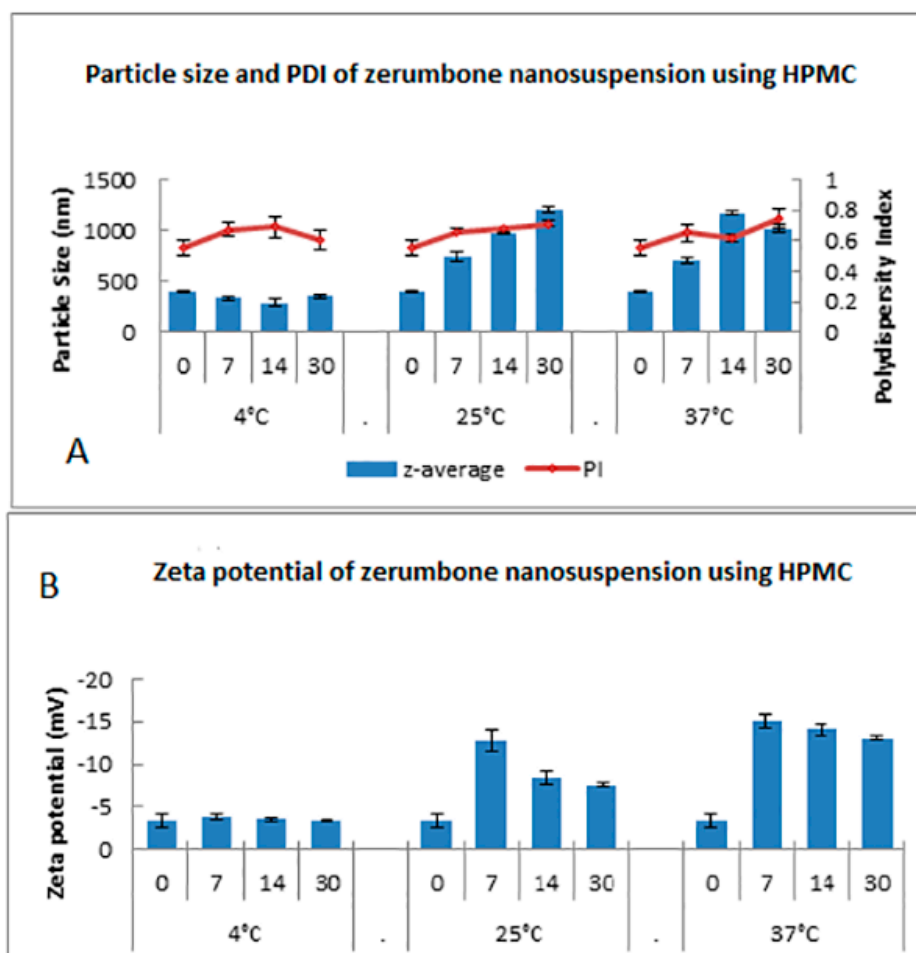

Figure 9. Short term stability profile of zerumbone nanosuspensions stabilized by SDS according to the days (0–30) stored at three different temperatures for (**A**) particle size & PDI; (**B**) Zeta potential.

4.3.2. Physical Stability of Zerumbone Nanosuspensions Stabilized by HPMC

The stability of the zerumbone nanosuspensions stabilized by HPMC at different temperatures was examined through the determination of the particle size, PDI, and ZP. Storage at 4 °C did not increase the particle size in contrast to storage at 25 °C and 37 °C (Figure 10). This indicates that there was no aggregation of the nanosuspensions when the samples were stored at 4 °C, while the nanosuspensions showed aggregation when stored at 25 °C or 37 °C. This is unsurprising, as the

nanosuspension storage at 25 °C and 37 °C may cause aggregation because of the increase in the kinetic energy of diffusing particles, which may overcome the energy barrier of electrostatic and/or steric repulsion [16]. Thus, based on particle size, the nanosuspensions stored at 4 °C are physically stable. The monodispersed samples possess a size distribution ranging from 0.01 to 0.7, while samples with a broad size distribution have values > 0.7 [18]. Based on the results, the general PDI indicates that it is monodispersed as the PI value was in between 0.5–0.7 (Figure 10). However, there is a noticeable increasing PI trend for 25 °C and 37 °C which may be due to the presence of large particles.

Figure 10. Short term stability profile of zerumbone nanosuspensions stabilized by HPMC according to the days (0–30) stored at three different temperatures for (**A**) particle size & PDI; (**B**) Zeta potential.

4.4. Saturation Solubility

As a result of the substantial reduction in the size of the crystals, as well as a possible amorphous nature of the crystals, solubility is likely to improve because of the increase in the surface area. The concentration readings were derived from the absorbance at 254 nm using the standard calibration curve. The zerumbone solution displayed solubility of 17.85 ± 1.52 μg/mL whereas the zerumbone nanosuspensions using SDS or HPMC stabilizers showed a solubility of 26.8 ± 3.88 and 32.11 ± 1.17 μg/mL respectively. This shows that the solubility of the nanosuspensions was increased by almost 2-fold as compared to the unprocessed zerumbone.

4.5. In Vitro Dissolution Study

The dissolution profile study was based on the method from the United States Pharmacopeia (USP). The dissolution profile of crude zerumbone was compared with the zerumbone

nanosuspensions prepared using the SDS or HPMC stabilizers (Figure 11A,B). The drug release from nanosuspensions using SDS was almost twice its counterpart (54.59% $\pm$ 7.34 vs. 31.92% $\pm$ 1.20) and results were statistically significant ($p < 0.05$). The zerumbone nanosuspensions prepared using HPMC showed a higher percentage of drug released as compared to the crude zerumbone (75.04% $\pm$ 2.17 vs. 31.92% $\pm$ 1.20) and the results were statistically significant ($p < 0.05$). These observations indicate an improved dissolution profile of zerumbone after the nanosizing process. The increased saturation solubility and dissolution rate will most probably increase the drug's bioavailability [11].
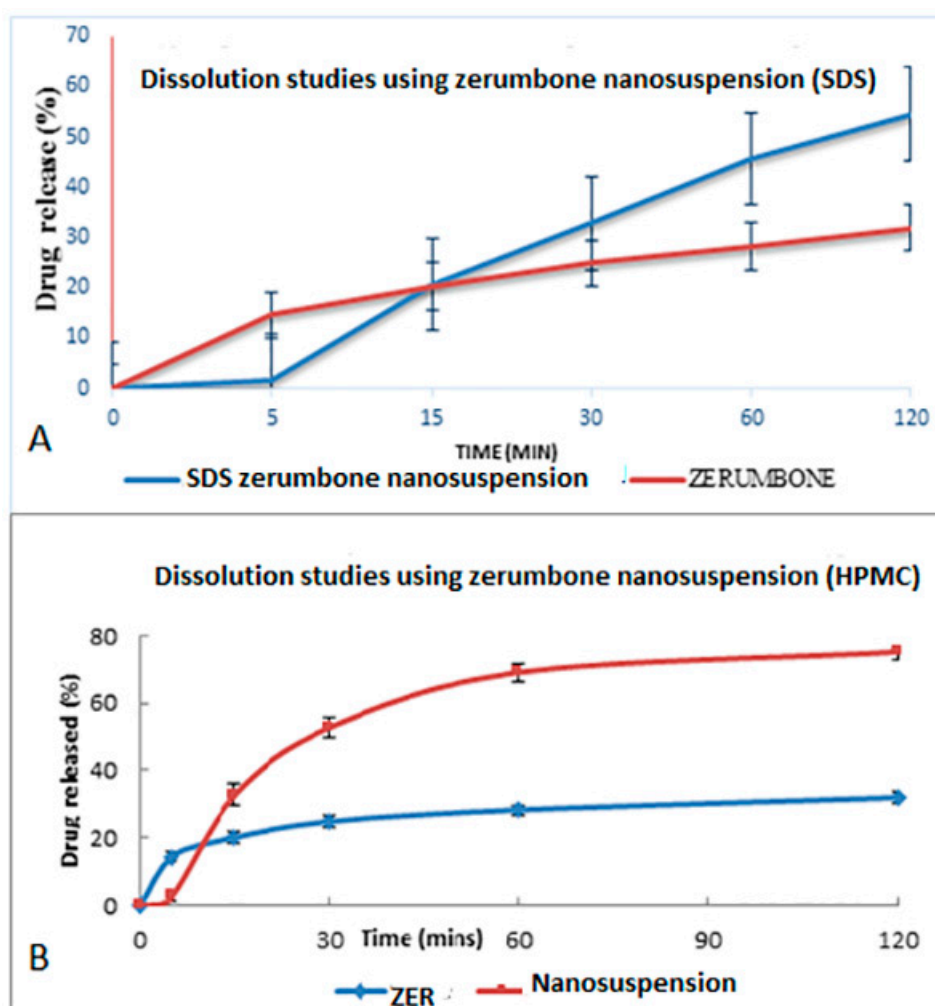
Figure 11. Dissolution profile of (**A**) freeze dried nanosuspension stabilized by SDS and (**B**) freeze dried nanosuspension stabilized by HPMC in a phosphate buffer pH 7.4 at 37 °C.

5. Conclusions

The current study focused on the development and in vitro evaluation of the zerumbone nanosuspensions. An optimised formulation showed a good reduction in the particle size and showed a short-term stability. Dissolution and saturation solubility studies demonstrated the ability of freeze-dried zerumbone nanosuspensions to enhance the dissolution rate and solubility of the drug compared to its unprocessed form.

Author Contributions: S.M. and L.A.C. conceived and designed the experiments; B.C.MK., S.J. and D.J.PD. performed the experiments. M.P. analyzed the data; S.M. contributed reagents/materials/analysis tools; S.M. and M.P. wrote the paper.

Conflicts of Interest: The authors declare no conflict of interest.

References

1. World Health Organization (WHO). Summary of WHO guidelines for the assessment of herbal medicines. *Herb. Gram.* **1993**, *28*, 13–14.

2. Bhuiyan, M.N.I.; Chowdhury, J.U.; Begum, J. Chemical investigation of the leaf and rhizome essential oils of *Zingiber zerumbet* (L.) Smith from Bangladesh. *Bangladesh J. Pharmacol.* **2008**, *4*, 9–12. [CrossRef]

3. Kitayama, T.; Okamoto, T.; Hill, R.K.; Kawai, Y.; Takahashi, S.; Yonemori, S.; Yamamoto, Y.; Ohe, K.; Uemura, S.; Sawada, S. Chemistry of Zerumbone. 1. Simplified Isolation, Conjugate Addition Reactions, and a Unique Ring Contracting Transannular Reaction of Its Dibromide. *J. Org. Chem.* **1999**, *64*, 2667–2672. [CrossRef] [PubMed]

4. Hall, S.; Nimgirawath, S.; Raston, C.; Sittatrakul, A.; Thadaniti, S.; Thirasasana, N.; White, A. Crystal structure of zerumbone [(E,E,E)-2,6,9,9-Tetramethylcycloundeca-2,6,10-trien-1-one]. *Aust. J. Chem.* **1981**, *34*, 2243. [CrossRef]

5. Abdul, A.B.; Abdelwahab, S.I.; Al-Zubairi, A.S.; Elhassan, M.M.; Murali, S.M. Anticancer and Antimicrobial Activities of Zerumbone from the Rhizomes of Zingiber zerumbut. *Int. J. Pharmacol.* **2008**, *4*, 301–304. [CrossRef]

6. Sidahmed, H.M.A.; Hashim, N.M.; Abdulla, M.A.; Ali, H.M.; Mohan, S.; Abdelwahab, S.I.; Taha, M.M.E.; Fai, L.M.; Vadivelu, J. Antisecretory, Gastroprotective, Antioxidant and Anti-*Helicobcter Pylori* Activity of Zerumbone from *Zingiber zerumbet* (L.) Smith. *PLoS ONE* **2015**, *10*, e0121060. [CrossRef] [PubMed]

7. Rahman, H.S.; Rasedee, A.; Yeap, S.K.; Othman, H.H.; Chartrand, M.S.; Namvar, F.; Abdul, A.B.; How, C.W. Biomedical properties of a natural dietary plant metabolite, zerumbone, in cancer therapy and chemoprevention trials. *Biomed. Res. Int.* **2014**, *2014*, 920742. [CrossRef] [PubMed]

8. Rabinow, B.E. Nanosuspensions in drug delivery. *Nat. Rev. Drug Discov.* **2004**, *3*, 785–796. [CrossRef] [PubMed]

9. Yadollahi, R.; Vasilev, K.; Simovic, S. Nanosuspension Technologies for Delivery of Poorly Soluble Drugs. *J. Nanomater.* **2015**, *2015*, 1–13. [CrossRef]

10. Shegokar, R.; Müller, R.H. Nanosuspensions: Industrially feasible multifunctional formulation technology for poorly soluble actives. *Int. J. Pharm.* **2010**, *399*, 129–139. [CrossRef] [PubMed]

11. Liversidge, G.G.; Cundy, K.C. Particle size reduction for improvement of oral bioavailability of hydrophobic drugs: I. Absolute oral bioavailability of nanosuspensionline danazol in beagle dogs. *Int. J. Pharm.* **1995**, *125*, 91–97. [CrossRef]

12. Müller, R.H.; Möschwitzer, J.; Bushrab, F.N. Manufacturing of Nanoparticles by Milling and Homogenization Techniques. In *Nanoparticle Technology for Drug Delivery*; CRC Press: Boca Raton, FL, USA, 2006; pp. 45–76.

13. Lipinski, C.A. Drug-like properties and the causes of poor solubility and poor permeability. *J. Pharmacol. Toxicol. Methods* **2000**, *44*, 235–249. [CrossRef]

14. Pharmaceutical Nanosuspensions for Medicament Administration as Systems with Increased Saturation Solubility and Rate of Solution. U.S. Patent No. 5,858,410, 1999. Available online: https://patents.google.com/patent/US5858410A/en (accessed on 27 July 2015).

15. Verma, S.; Huey, B.D.; Burgess, D.J. Scanning Probe Microscopy Method for Nanosuspension Stabilizer Selection. *Langmuir* **2009**, *25*, 12481–12487. [CrossRef] [PubMed]

16. Verma, S.; Kumar, S.; Gokhale, R.; Burgess, D.J. Physical stability of nanosuspensions: Investigation of the role of stabilizers on Ostwald ripening. *Int. J. Pharm.* **2011**, *406*, 145–152. [CrossRef] [PubMed]

17. Kipp, J. The role of solid nanoparticle technology in the parenteral delivery of poorly water-soluble drugs. *Int. J. Pharm.* **2004**, *284*, 109–122. [CrossRef] [PubMed]

18. Mishra, P.R.; Al Shaal, L.; Müller, R.H.; Keck, C.M. Production and characterization of Hesperetin nanosuspensions for dermal delivery. *Int. J. Pharm.* **2009**, *371*, 182–189. [CrossRef] [PubMed]

19. Dev, S. Studies in sesquiterpenes—XVI: Zerumbone, a monocyclic sesquiterpene ketone. *Tetrahedron* **1960**, *8*, 171–180. [CrossRef]

20. Rasedee, A.; Abdul, A.B.; Zeenathul, N.A.; Rahman, H.; Yeap, S.; Wan Ghani, W.N.H.; Othman, H.H.; How, C.W. Zerumbone-loaded nanostructured lipid carrier induces G2/M cell cycle arrest and apoptosis via mitochondrial pathway in a human lymphoblastic leukemia cell line. *Int. J. Nanomed.* **2014**, *9*, 527. [CrossRef] [PubMed]

21. Ravichandran, R. In vivo pharmacokinetic studies of albendazole nanoparticulate oral formulations for improved bioavailability. *Int. J. Green Nanotechnol. Biomed.* **2010**, *2*, 46–53.